Analyzing Radio Scattering Caused by Various Building Elements Using mm-Wave Scale Model Measurements and Ray-Tracing

Published Version:
E. M. Vitucci, J.C. (2019). Analyzing Radio Scattering Caused by Various Building Elements Using mm-Wave Scale Model Measurements and Ray-Tracing. IEEE TRANSACTIONS ON ANTENNAS AND PROPAGATION, 67(1), 665-669 [10.1109/TAP.2018.2876716].

Availability:
This version is available at: https://hdl.handle.net/11585/646754 since: 2021-11-02

Published:
DOI: http://doi.org/10.1109/TAP.2018.2876716

Communication

Analyzing Radio Scattering Caused by Various Building Elements Using mm-Wave Scale Model Measurements and Ray-Tracing

E. M. Vitucci, *Senior Member, IEEE*, J. Chen, *Student Member, IEEE*, V. Degli-Esposti, *Senior Member, IEEE*, J. Lu, *Member, IEEE*, H. L. Bertoni, *Life Fellow, IEEE*, and X. Yin, *Member, IEEE*

***Abstract*—Interaction of UHF radio waves with a typical office building and the resulting scattering characteristics are studied in this work using mm-wave frequency measurements and ray tracing simulations on a scale model of the building. A "disaggregation approach" is followed to separately test different structural elements (façade, internal structure, furniture) and to separately simulate different interaction mechanisms (specular reflection, edge diffraction, transmission, diffuse scattering) thus achieving a deeper understanding of the propagation process. Results suggest that scattering from buildings can be modeled neglecting the internal structure of the building, but proper modeling of non-specular propagation is necessary, even with a controlled and completely known environment such as the scale building model.**

***Index Terms*—Buildings, Millimeter wave, UHF, Diffraction, Scattering, Ray Tracing, Urban Propagation.**

I. Introduction

Radio propagation in urban environments has been widely studied over the last decades using both empirical and physics-based approaches. Nevertheless, the propagation mechanisms characterizing scattering from buildings, which lay at the base of urban radio propagation, have not been fully understood yet. A few studies have addressed scattering from buildings by separating specular reflection from diffuse scattering due to surface roughness and minor construction details, and modeling the latter using Heuristic models, such as the Effective Roughness (ER) model [1], [2] or variants of it [3]. Other studies have applied electromagnetic methods for calculating scattering from building façades [4], [5]. In [3] a realistic building scale model was used to deconstruct the building into different parts (façade, inner walls and floors, furniture) and investigate the impact of each one of them on the overall back-scattering process. Nevertheless, basic questions are still partly unanswered. For example: (a) what ray interactions, such as specular reflection, edge diffraction, transmission and diffuse scattering, are involved; (b) how many interactions along a ray path must be included; (c) is non-specular (diffuse) scattering really so important as highlighted in previous work [1] even when the electromagnetic and geometrical characteristics of the building are completely known and under control; and (d) what are the 3D building scattering characteristics, including the transmission through the building (forward scattering), and the case where the transmitter or receiver is not near the horizontal plane? This last question is important when characterizing air-to-ground radio links, such as found in GPS systems, drone communications, and remote sensing.

Similarly to other works where urban propagation has been studied with the aid of scale models [6], in the present study we address the foregoing questions for real systems operating at around 2 GHz by calibrating our ray tracing tool against scattering measurements made at 60 and 70 GHz on a scale building model. The measurements include previously reported back scattering results [3], as well as new measurements for transmission through the building. Thanks to the use of the modular building model we have been able to separately measure scattering from the different parts of the building. On the other hand, thanks to RT simulations where we can separately enable different propagation mechanisms such as specular reflection, diffraction, diffuse scattering, transmission, and different combinations of them, we have been able to separately analyze the role and importance of different propagation processes. Results confirm previous findings that scattering in the backward half space is dominated by the contribution of the front façade of the building, and only a minor contribution comes from back-scattering from the building interior.

RT simulations with enough interactions per ray (e.g. eight reflections, three diffractions and one diffuse scattering) accurately match measurements. However, for best results a somewhat higher diffuse scattering parameter (S = 0.4), as defined in Section III, is required as compared to the value (S = 0.25) found for a uniform slab of the plywood used to build the model [7]. This value may be needed to account for roughness of the cut edges of the plywood in the model.

When trying to reproduce real building scattering using a simplified geometrical description of the buildings (e.g. ESRI SHAPE-format) where windows and construction details are disregarded [2], diffuse scattering must compensate for the absence of edge diffraction and multiple reflections. In this case a scattering parameter of larger value (S = 0.6) must be used.

Transmission through a building corresponds to scattering

This work is jointly supported by the International Exchange Program for Graduate Students, Tongji University, the Natural Science Foundation of China (NSFC) under Grant No. 61471268, the HongKong, Macao & Taiwan Science Technology Cooperation Program of China, and the European COST Action CA15104 IRACON.

Enrico M. Vitucci and V. Degli-Esposti are with the Dipartimento di Ingegneria dell'Energia Elettrica e dell'Informazione "Guglielmo Marconi" (DEI), IT-40136 Bologna, Italy. (email:enricomaria.vitucci@unibo.it; v.degliesposti@unibo.it).

J. Chen and X. Yin are with the College of Electronics and Information Engineering, Tongji University, Shanghai 201804, China. (email: 09chenjiajing@tongji.edu.cn; yinxuefeng@tongji.edu.cn).

J. Lu is with Polaris Wireless, inc., Mountain View, CA 94043, USA. (email:jlu@polariswireless.com).

H.L. Bertoni is with the NYU Wireless Center at Tandon School of Engineering, New York University, Brooklyn NY, 11215 USA (email: hb752@nyu.edu)

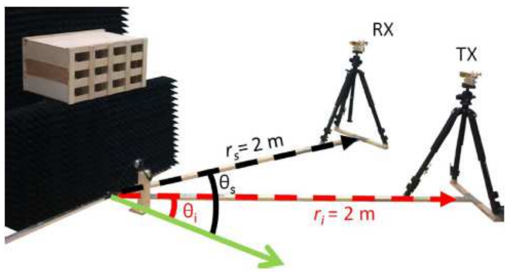

Fig. 1. Quasi-anechoic, 60 GHz measurement setup.

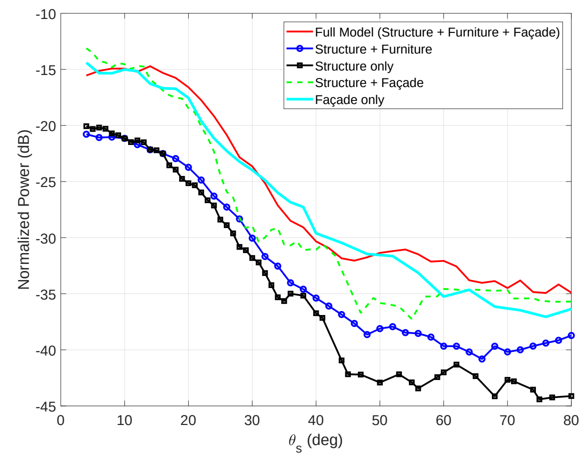

Fig. 2. Angular averaged measurements at 60 GHz (backward half-space, 10° incidence).

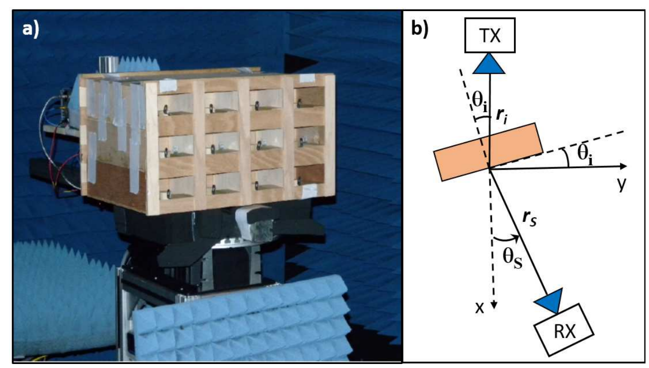

Fig. 3. a) Photograph of the anechoic room measurements; b) Representation of the measurement setup (2D top view).

in the forward half space. This scattering is dominated by multiple transmissions and multipath components generated by the building interior, with furniture playing a major role. Since we could not accurately model furniture scattering in our RT simulator, we again used a large value (S = 0.6) of the forward scattering parameter for transmission through walls to achieve reasonable comparison with measurements.

In the following, Section II describes the measurement equipment and procedure. Section III presents results obtained by both measurements and simulations. Finally, conclusive remarks are addressed in Section IV.

II. Scale model measurements

The office building scale model which was initially presented in [3] has three parts, 1) external building façade with window openings; 2) internal building structure; 3) office furniture. Because ordinary window glass is thin compared to wavelength at 2 GHz, and therefore highly transmitting, for the model the windows were left open. The size of the structure and furniture were all built using a 1/30 scale to model 2 GHz propagation at 60 GHz. Also, the model's walls were all made from plywood slabs because of their similar reflectivity and transmissivity characteristics at 60 GHz to real building walls at 2 GHz [3].

Backscattering measurements were initially performed at 60 GHz using different configurations of the scale building model (e.g., no façade + building structure + no furniture = structure only) [3]. The transmitter (Tx) and receiver (Rx) antennas were at the same distance (2 m) from a common rotation axis on the façade of the model, as depicted in Fig. 1. To perform scattering measurements for a specific incident angle θ_i, the Tx antenna was placed at the desired θ_i, while the Rx antenna was rotated through different θ_s. An example for $\theta_i = 10°$ and different configurations of the building model is shown in Fig. 2. Here, the power has been normalized with respect to the specular reflection from a metal sheet, and smoothed using a sliding window of 12°. From the figure it is quite evident that the backscattered power of the full building model is dominated by the backscattering of the façade, while the contribution from the internal structure and furniture is relatively minor.

Transmission and forward scattering measurements were also performed on the building model at Ilmenau University of Technology, Germany, at a slightly different frequency of 70 GHz using a state-of-the-art setup [8]. Since the electromagnetic characteristics of most materials at 60 and 70 GHz are similar [9], the different carrier frequency shouldn't significantly change the scattering pattern. Therefore these measurements can be considered a completion of the previous 60 GHz measurements to get a complete scattering characterization. In the forward scattering measurements, a rotating positioner and properly located absorbers were used in the anechoic chamber as shown in Fig. 3. The Rx was rotated in the forward half-space of the model, and the scattering angle θ_s was measured with respect to the transmission direction. The Tx was kept fixed, and different incidence angles θ_i were considered by tilting the building model with respect to the xy coordinates system shown in Fig. 3b).

III. Results

In this Section, the properties of scattering from the scale building model are analyzed through comparisons between measurements and RT simulations. We used an advanced 3D RT tool which includes also diffuse scattering, modelled using the ER approach [1], [10], where walls are divided into surface elements (tiles) [11], [12], and non-specular interactions generated by surface roughness, internal irregularities and also micro-interactions from minor building elements (columns, decorations etc.) are modelled using an average scattering pattern for each tile.

The diffuse scattering intensity relative to specular reflection and transmission is given by the scattering parameter S. The scattering parameter and the scattering pattern are generally different for the backward half space (Tx and Rx located on the same side with respect to the wall) and the forward half space (Tx and Rx located at opposite sides). The intensity of the diffuse field at the Rx is given by [1], [10]:

$$E_s^{(Rx)} = \begin{cases} \frac{A}{r_i r_s} \cdot S_R \cdot \left(\frac{1+\cos\psi_R}{2}\right)^{\frac{\alpha_R}{2}} & \text{backward half-space} \\ \frac{A}{r_i r_s} \cdot S_T \cdot \left(\frac{1+\cos\psi_T}{2}\right)^{\frac{\alpha_T}{2}} & \text{forward half-space} \end{cases} \quad (1)$$

where S_R (S_T) is the scattering parameter in the backward (forward) half space, ψ_R (ψ_T) is the angle between the scattering direction and the specular reflection (transmission), α_R (α_T) is a parameter related to the width of the scattering lobe, r_i (r_s) is the distance between the scattering tile and Tx (Rx), and A is a normalization factor depending on the incidence direction and the intensity of the field emitted by the Tx antenna. In order to satisfy the power balance, and therefore the physical soundness of the model, the power of specular reflection (transmission) is also reduced by a factor [1], [10]:

$$R = \begin{cases} \sqrt{1-S_R^2} & \text{backward half-space} \\ \sqrt{1-S_T^2} & \text{forward half-space} \end{cases} \quad (2)$$

In RT simulations, the scale model was digitized into a map where the façade and internal walls were modelled through dielectric slabs, i.e. rectangular layers with a proper thickness. The furniture objects - metal chairs, table, desk, bookcase and light fixtures, see Fig. 4 - were modelled in a deterministic way considering their location, geometry, and the type of material. Curved surfaces (table, light fixtures) were approximated through rectangular and triangular facets. Metal chairs and light fixtures were modelled as Perfectly Electrical Conductors (PEC).

The kind of Plywood we used has a mild roughness surface with deviations vs. a smooth surface well below 1 millimeter, i.e. a small fraction of a wavelength at 60 GHz. This is similar to most real-world building walls at 2 GHz, where surface deviations are below 1 cm vs. a wavelength of 15 cm. Therefore RT simulations should require similar diffuse scattering parameters settings at the two frequencies for the scale model and for a real building.

The following dielectric material parameters were used in RT simulation for building walls and wooden objects: $\epsilon_r = 2,\ \sigma = 0.3\ S/m$. These correspond to average values for plywood slabs found in [7] and [9] and yield reflectivity and transmissivity figures similar to those of a brick wall at 2 GHz [3]. This fact is important in order for the scale model to behave in a similar way as a real building in terms of scattering. For instance, using the parameter values above we get an through-wall attenuation of about 3.5 dB for the 0.5 cm thick plywood slabs, which is similar to the attenuation of a brick wall at 2 GHz.

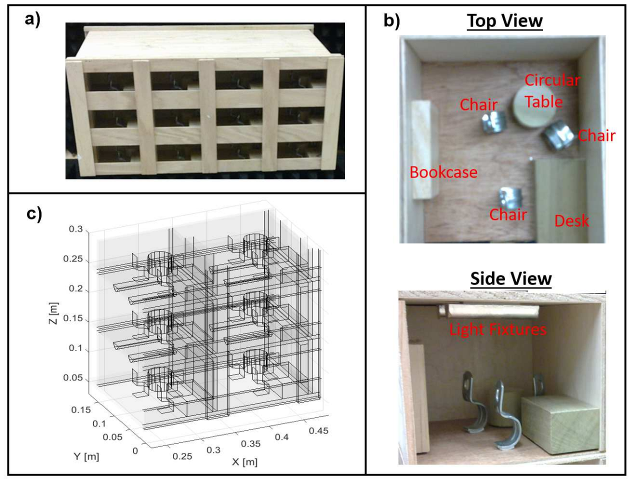

Fig. 4. a) Full building model including façade and furniture; b) Detail of the furniture; c) Representation of the geometrical model used in RT simulation.

A picture of the complete building model including façade and furniture, and a sketch of the corresponding geometrical model used in RT simulation, are shown in Fig. 4.

In order to apply the ER model walls are discretized into 2x2 cm tiles, and a directive scattering lobe with $\alpha = 4$ was applied to each tile. The RT simulations were performed with a detailed representation of the measurement setup, including the 3D radiation patterns of the antennas. To determine the appropriate value of the scattering coefficients, a least-square problem is solved which minimizes the root-mean-square-error (RMSE) of simulated received power and the measurement results. Readers may refer to [13] for the detailed description of the simulator.

Using RT, a full simulation of the 3D scattered power by any object is possible. As an example, in Fig. 5 we show the simulated 3-dimensional scattering pattern for the full building model, considering a directive Tx antenna pointed towards the center of the building façade, with an incidence angle of $10°$ with respect to the normal, and several Rx positions located on a spherical surface with 2 m radius, centered on the building model. As expected, the highest levels of received power are in the backscattering half-space and the maximum value is obtained when Rx has the same height as Tx and the scattering angle corresponds to the specular reflection angle; the received power rapidly decreases when Rx height becomes lower or higher than the Tx height. For Rx locations on the opposite side of Tx with respect to the building, transmissions and forward scattering take place: in this case we observe that the received power becomes generally more spread, not only in the azimuthal plane but even for lower and higher elevation angles, compared to the back-scattering half-space. When the Rx is located at the top or the bottom of the building model, the received power is much lower than for other positions. This is due to the very low level of power backscattered from the ceilings, since the Tx mainly illuminates the vertical walls.

In the following, a detailed analysis is done only for Rx

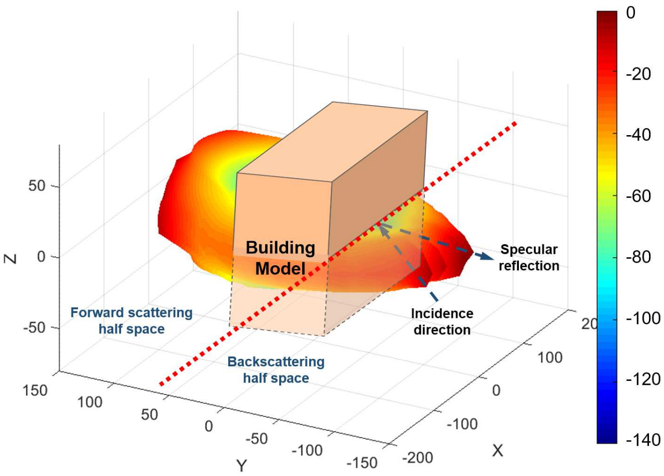

Fig. 5. The simulated 3D received power pattern at 60 GHz.

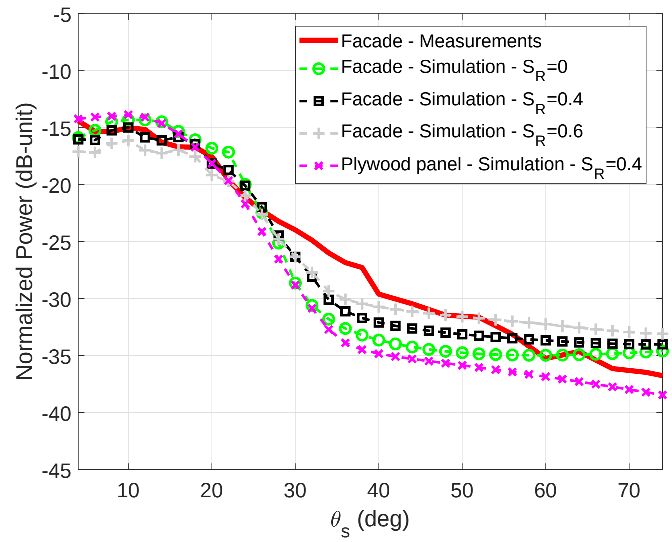

Fig. 6. Comparison between measurements and RT simulations for the building façade (backward half space, $f = 60\,GHz$).

located at the same height, taking the measurements at 60 GHz and 70 GHz as a reference to investigate the main propagation mechanisms and to validate the ER diffuse scattering model. The same power normalization and smoothing used for the measured curves has been applied to RT simulations.

A. Performance evaluation for the backscattering case

Fig. 6 illustrates a comparison between RT simulations and measurements at 60 GHz in the backward half space for the building façade for $\theta_i = 10°$. Backscattering from the building façade is dominated by a few specular reflections from the vertical and horizontal slabs surrounding the windows, and diffractions at the edges of the vertical slabs. Due to the complex structure of façade, up to 3 interactions are necessary in order to reproduce with good accuracy the scattering mechanism. Diffraction is modelled according to the Uniform Theory of Diffraction (UTD), and heuristically modified UTD coefficients have been used [14] to simulate the power diffracted by dielectric wedges.

With this settings, the RT simulation can match the measured power levels both in the specular region and in the tail. Nevertheless, to have a better match in the "transition region" diffuse scattering is also needed, and a best value of $S_R = 0.4$ (i.e. about 15% of the power) has been found (black curve). Higher S_R values (e.g. 0.6) are not suitable, because the power is overestimated too much in the tail, and underestimated in the specular region (light gray curve), due to reduction of the reflected and diffracted components to satisfy the power balance. $S_R = 0.4$ is a bit higher compared to the values suggested in [7], where a maximum value of 0.25 has been found for a flat plywood panel at millimeter wave frequencies. The higher value of $S_R = 0.4$ is thought to account for irregularities of the cut edges of the plywood that are not modeled, and for possible multiple interactions that may have been omitted due to approximations made in the geometrical model of the façade. In any case, for scattering angles between 30° and 40°, the computation using $S_R = 0.4$ still underestimates the observed scattering. This discrepancy may be due to scattering from the additional mounting clamps and frame used support the façade when it was measured by itself.

It is interesting to see that simulations for a flat uniform plywood panel of the same overall dimensions of the façade (pink curve in Fig. 6) over estimates the specular reflection but underestimates the scattering at high angles. To achieve a better comparison with measurements, a uniform panel must have a higher value $S_R = 0.6$, as found in [3], which corresponds to diffuse scattering carrying about 36% of the total back-scattered power.

A comparison between the measured and computed backscattering for the full building model is shown in Fig. 7. Up to 8 reflections, 3 diffractions, 1 diffuse scattering and combinations with unlimited transmissions on internal walls have been considered here, in order to get a realistic simulation of the complex multi-bounce propagation mechanisms that takes place inside the full building model. Compared to the façade only case, it is even more evident that some scattering is needed to match the measured curve: the simulation without scattering ($S_R = 0$, green curve) is not realistic in this case, because power is overestimated in the specular region and underestimated in the tail. By applying the ER model, the agreement is quite good in this case, and the best S_R value is again 0.4 (black curve) as found for the façade, thus confirming that backscattering from the full building model is dominated by the façade. In Fig. 7 the simulated power of the plywood panel (with $S_R = 0.6$) is also reported as a reference (blue curve): it is interesting to note that this curve also matches quite well the measurements, but in the transition region the performance is poorer compared to the full simulation. The explanation for this is that the internal structure of the building, including furniture, probably has some influence on the received power in the "transition" region between the specular zone and the tail.

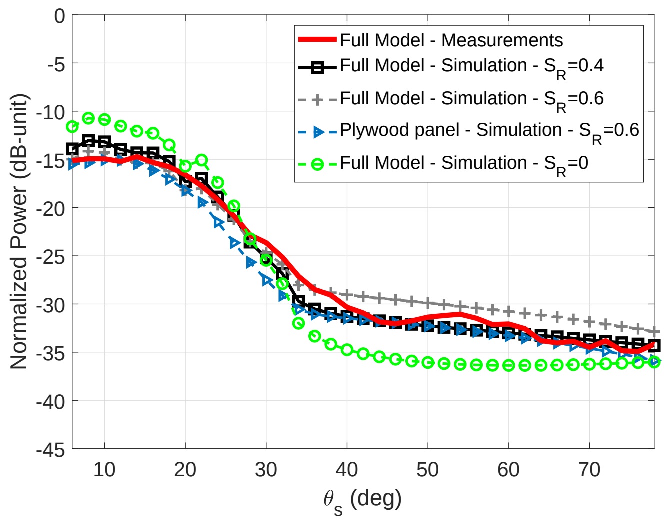

Fig. 7. Comparison between measurements and RT simulations for the full building model (backward half space, $f = 60\,GHz$).

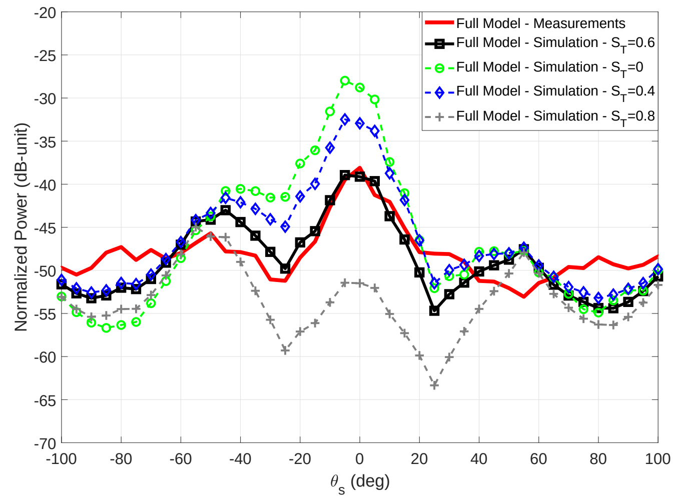

Fig. 8. Comparison between measurements and RT simulations for the full building model in the forward half space ($\theta_i = 0°$, $f = 70\,GHz$).

B. Performance evaluation for the forward scattering case

In Fig. 8, 9, we show the comparison between the RT simulations and measurements at 70 GHz in the forward half space, for the full building model. According to the measurement setup shown in Fig. 3b), two different incidence angles have been considered: $\theta_i = 0°, \theta_i = 10°$, with results shown in Fig. 8, 9, respectively. Measurements were made for larger values of θ_i, but are not shown here since for these cases Tx also illuminated the sidewalls of the building, and so do not clearly show the effects of transmission through the building.

In RT simulations, the candidate values of S_T are chosen from [0, 0.4, 0.6, 0.8], and the same settings of the backscattering case have been considered for the coherent interactions. From the plots, it is evident that the best-match scattering coefficient value is $S_T = 0.6$, which means that about 36% of the incident power is diffused. With $S_T = 0$, the agreement is unsatisfactory because the simulated power is highly overestimated in the transmission peak and for intermediate scattering angles, and underestimated for grazing scattering angles. Increasing the S_T value, the transmission peak is attenuated - due to the power balance - and the power distribution become more spread, similarly to the measurements. If S_T is further increased (e.g. to 0.8), the behaviour becomes unrealistic because the transmission peak is attenuated too much.

This result partly agrees with what shown in [10], [7], where a higher scattering parameter value is suggested for forward scattering compared to backscattering, even for simpler scattering samples like dielectric slabs and building walls. In the case considered here the S_T value is obviously higher, because the considered sample - i.e. the full building model - is much more complex. In particular, the high value of the scattering parameter suggests that forward scattering is essentially dominated by multiple transmissions and scattering from the building interior, where a major role is played by furniture. Since in the simulation the geometrical model of the furniture objects cannot be very accurate, considering only coherent interactions like specular reflections and diffractions some multipath components might be missing in the simulations, and therefore the ER diffuse scattering model probably has to compensate also for this effect.

It is worth noting that the ER model has been validated and parameterized in the present work for the first time in the forward half-space. The full building model, including façade, partitioning walls and furniture, can be considered representative of typical mid-size commercial and residential buildings. Therefore, thanks to the scaling technique, RT simulations on the building model at $60\,GHz$ will show the same performance and will require the same diffuse scattering parameter values ($S_R = 0.4$, $S_T = 0.6$) as RT simulations on full-size buildings of the same kind at UHF frequencies. However, if buildings are represented in a simplified way as polygonal prisms without any architectural detail, which is the case for most ESRI-SHAPE format urban databases, higher values should be used to compensate for the absence of such scattering-generating details, for example $S_R = 0.6$ as used in [2].

IV. Conclusions

Comparing measurements in Fig. 2 and simulations in Fig. 6, 7 for the façade by itself and for the complete building, it is seen that the façade is the primary source of specular reflection and non-specular scattering from a building. Specular reflection is readily modeled as coming from a flat surface by appropriate choice of the reflection coefficient. When using ray tracing to predict non-specular scattering, even for this simple structure, it was found necessary to account for the shape of the façade in 3D and for irregularity of its surface. Real buildings with rough surfaces, metal window frames, balconies, etc., will be even more difficult to evaluate theoretically. However a simple representation of the non-specular scattering can be achieved using a uniformly random surface, as seen from the "Plywood panel - simulations" for $S_R = 0.6$

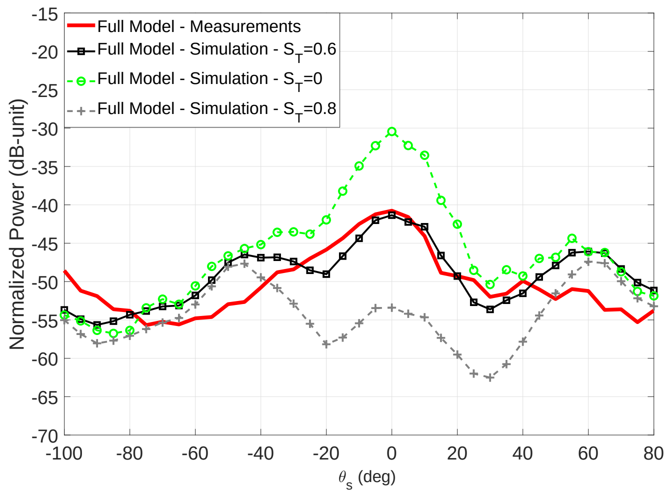

Fig. 9. Comparison between measurements and RT simulations for the full building model in the forward half space ($\theta_i = 10°$, $f = 70\,GHz$).

in Fig. 7. Transmission through the buildings involves a high degree of scattering due to the presence of internal walls and furniture, and cannot be accurately modeled using ray tracing without the ad-hoc addition of strong scattering: for this reason, a high value of the forward scattering parameter ($S_T = 0.6$) is needed to match the measurements, as shown in Fig. 8, 9.

V. Acknowledgements

The Authors would like to thank Professor Reiner Thomä and his group from Ilmenau University of Technology for helping us carry out measurements in their anechoic chamber, and the graduate students Ferrino Fantini and Marco Vanucci for their help in preparing the input data of ray tracing simulations.

References

[1] V. Degli-Esposti, F. Fuschini, E. M. Vitucci, and G. Falciasecca, "Measurement and modelling of scattering from buildings," *IEEE Trans. Antennas Propagat*, vol. 55, no. 1, pp. 143–153, Jan 2007.

[2] E. M. Vitucci, F. Mani, V. Degli-Esposti, and C. Oestges, "Polarimetric properties of diffuse scattering from building walls: Experimental parameterization of a ray-tracing model," *IEEE Trans. Antennas Propagat*, vol. 60, no. 6, pp. 2961–2969, June 2012.

[3] J. S. Lu, H. L. Bertoni, and V. Degli-Esposti, "Scale model investigation of mechanisms for scattering from office buildings at 2 GHz," *IEEE Trans. Antennas Propagat*, vol. 62, no. 12, pp. 6435–6442, Dec 2014.

[4] Y. B. Ouattara, S. Mostarshedi, E. Richalot, J. Wiart, and O. Picon, "Near- and far-field models for scattering analysis of buildings in wireless communications," *IEEE Trans. Antennas Propagat*, vol. 59, no. 11, pp. 4229–4238, Nov 2011.

[5] P. Pongsilamanee and H. L. Bertoni, "Specular and nonspecular scattering from building facades," *IEEE Trans. Antennas Propagat*, vol. 52, no. 7, pp. 1879–1889, July 2004.

[6] D. Erricolo, G. D'Elia, and P. L. E. Uslenghi, "Measurements on scaled models of urban environments and comparisons with ray-tracing propagation simulation," *IEEE Trans. Antennas Propagat*, vol. 50, no. 5, pp. 727–735, May 2002.

[7] F. Fuschini, S. Häfner, M. Zoli, R. Müller, E. M. Vitucci, D. Dupleich, M. Barbiroli, J. Luo, E. Schulz, V. Degli-Esposti *et al.*, "Item level characterization of mm-wave indoor propagation," *EURASIP Journal on Wireless Communications and Networking*, vol. 2016, no. 1, pp. 1–12, Jan 2016.

[8] R. Müller, S. Häfner, D. Dupleich, and J. Luo, "Ultra-wideband channel sounder for measurements at 70 GHz," in *2015 IEEE 81st Vehicular Technology Conference (VTC2015-Spring)*, May 2015, pp. 1–5.

[9] S. Salous, V. Degli-Esposti, F. Fuschini, R. S. Thomä, R. Müller, D. Dupleich, K. Haneda, J. M. M. Garcia-Pardo, J. P. Garcia, D. P. Gaillot, S. Hur, and M. Nekovee, "Millimeter-wave propagation: Characterization and modeling toward fifth-generation systems. [wireless corner]," *IEEE Antennas Propag. Mag.*, vol. 58, no. 6, pp. 115–127, Dec 2016.

[10] F. Fuschini, V. Degli-Esposti, and E. M. Vitucci, "A model for forward-diffuse scattering through a wall," in *Proceedings of the 4th European Conference on Antennas and Propagation (EuCAP 2010)*, Apr 2010, pp. 1–4.

[11] V. Degli-Esposti, F. Fuschini, and E. M. Vitucci, "A fast model for distributed scattering from buildings," in *3rd European Conference on Antennas and Propagation (EuCAP 2009)*, Mar 2009, pp. 1932–1936.

[12] L. Tian, V. Degli-Esposti, E. M. Vitucci, and X. Yin, "Semi-deterministic radio channel modeling based on graph theory and ray-tracing," *IEEE Trans. Antennas Propagat*, vol. 64, no. 6, pp. 2475–2486, June 2016.

[13] F. Fuschini, E. M. Vitucci, M. Barbiroli, G. Falciasecca, and V. Degli-Esposti, "Ray tracing propagation modeling for future small-cell and indoor applications: A review of current techniques," *Radio Science*, vol. 50, no. 6, pp. 469–485, Jun 2015.

[14] P. D. Holm, "A new heuristic UTD diffraction coefficient for nonperfectly conducting wedges," *IEEE Trans. Antennas Propagat*, vol. 48, no. 8, pp. 1211–1219, Aug 2000.